

# The total suppression of light reflection from a one-dimensional photonic crystal by a two-dimensional array of nanoparticles

Sergey G. Moiseev,<sup>a\*</sup> Igor A. Glukhov,<sup>a</sup> Andrei A. Fotiadi<sup>b,c</sup>

<sup>a</sup> Kotelnikov Institute of Radioengineering and Electronics of the Russian Academy of Sciences, Moscow, Russia

<sup>b</sup> Electromagnetism and Telecommunication Department, University of Mons, Mons, B-7000, Belgium

<sup>c</sup> Optoelectronics and Measurement Techniques Unit, University of Oulu, 90570 Oulu, Finland

\*serg-moiseev@yandex.ru

## ABSTRACT

The possibility of strong modification of the reflection spectrum of a one-dimensional photonic crystal using a dilute two-dimensional array (monolayer) of metal nanoparticles is demonstrated. Using analytical and numerical methods, it is shown that the reflection of electromagnetic wave in the photonic bandgap range can be completely suppressed by nanoparticles located in the surface dielectric layer. In this case, the entire energy of the incident wave is absorbed by metal nanoparticles. The dependence of the absorption spectra of hybrid photonic structure on the array parameters is studied. The theoretical findings and predictions are verified by numerical simulation results. The obtained results can be used to create filters, polarizers and absorbers for predetermined frequencies in the visible and near-IR domains.

**Keywords:** photonic crystal, 2D array of nanoparticles, localized surface plasmon resonance, absorber

## INTRODUCTION

Noble metallic nanoparticles (NPs) can exhibit valuable properties such as localized surface plasmon resonance (LSPR), which can find various optoelectronic and photonic applications. The LSPR is based on the collective oscillation of electrons in individual NP and depends on its shape and size and the surrounding dielectric medium. Due to the LSPR, the large electro-magnetic field enhancement, absorption and scattering can occur [1-3]. The peak position and bandwidth of LSPR can be determined by the size, shape and geometry of NPs, which makes it tunable conveniently by controlling those structural factors of plasmonic NPs [4-6]. One of the unusual manifestations of plasmon resonance response is the resonant effective permittivity of metal-dielectric nanocomposites (3D arrays of NPs embedded in a host material), whereas the optical characteristics of the initial materials have no resonant features [7-10]. The well-established properties of NP arrays have been put to use in the last decades for the design of sensors [11], anti-reflection optical coatings [12,13], polarization-sensitive structures [6,8,14,15], filters and absorbers [6,12,16] with thickness less than light wavelength.

Enhanced light-matter interaction can be achieved by incorporating NPs into the photonic crystal structures, in particular into the microcavity formed by distributed Bragg reflectors (DBRs) [17-21]. The plasmonic absorber effect can be achieved using 2D arrays of nanoparticles that are embedded at position of the localization of the optical field inside microcavity [22-25]. When placing 2D NP arrays outside the microcavities a strong coupling of the photon and plasmon subsystems is greatly weakened. In this work, we show the possibility of strong modification of the spectral and absorption characteristics of a highly reflective structure such as distributed Bragg reflector (DBR) with the use of a 2D array of metallic NPs inside a surface dielectric layer (outside the microcavity).

## DESCRIPTION OF THE SYSTEM AND ANALYTICAL METHODS

We consider a complex structure composed of distributed Bragg reflector (DBR) and composite layer with 2D array of metallic NPs (Fig. 1). A unit cell of DBR is formed from layers of dielectric materials  $A$  and  $B$  with the thicknesses  $d_A$  and  $d_B$  and relative permittivities  $\varepsilon_A$  and  $\varepsilon_B$ , respectively. The thicknesses  $d_A$  and  $d_B$  satisfy the Bragg condition of resonant reflection at vacuum wavelength  $\lambda_{br}$ :

$$d_A \operatorname{Re}(\sqrt{\varepsilon_A}) = d_B \operatorname{Re}(\sqrt{\varepsilon_B}) = \lambda_{br} / 4. \quad (1)$$

The composite layer is formed from homogeneous dielectric material  $C$  with relative permittivity  $\varepsilon_c$  and an embedded 2D array of metallic NPs  $M$ . The array  $M$  is formed by identical metal NPs of spheroidal shape. This array divides layer  $C$  with the thickness  $d_C$  into two layers  $C_1$  and  $C_2$ . Layer  $C_2$  with the thickness  $d_2$  separates the NP array from DBR.

All NPs are identical and characterized by aspect ratio  $\xi = a_1/a_2$  ( $a_1 > a_2$ ), where  $a_1$  and  $a_2$  are the half-lengths of their polar and equatorial axes, respectively. The NPs are ordered in a periodic 2D array with a square unit cell whose period  $p$  is the interparticle distance. The polar axis of the NPs is parallel to the  $z$  axis of the Cartesian coordinate system ( $z$  axis is perpendicular to the interfaces of the DBR). Translational invariance is assumed along the  $x$  and  $y$  axes. The dimensions of the NPs are much smaller than the wavelength of the optical wave ( $\{2a_1, 2a_2\} \ll \lambda_0 / \sqrt{\varepsilon_c}$ ).

Thus, the entire hybrid structure is described by the formula  $C_1MC_2[AB]^N$ , where  $N$  is the number of periods of the DBR. It is surrounded by air, and we assume that an incident plane wave impinges under normal incidence on the left-hand side of the structure, at  $z = -d_C$  of a Cartesian coordinate system. The time dependence of the electromagnetic fields is taken as  $\exp(-i\omega t)$ , where  $\omega = 2\pi c/\lambda_0$  is the angular frequency of the incoming plane wave. The dimensions of the layers along the  $x$  and  $y$  axes are much larger than their thicknesses along the  $z$  axis, so that the boundary effects along the  $x$  and  $y$  directions are neglected.

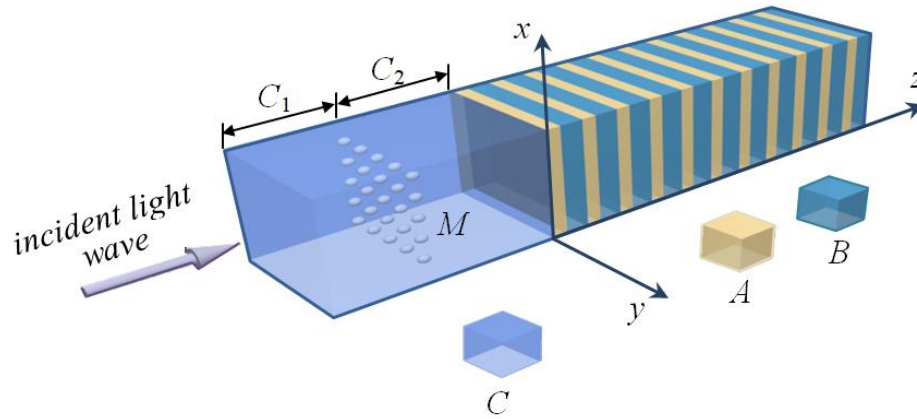


Figure 1. Schematic of the hybrid structure  $C_1MC_2[AB]^N$ : the surface layer  $C$  with embedded 2D array of NPs  $M$  is adjacent to the DBR  $[AB]^N$  with a unit cell formed from layers  $A$  and  $B$ . The 2D NP array is formed by identical metal NPs of ellipsoidal shape with polar axis parallel to the  $z$  axis.

In order to calculate the spectral characteristics of the complex photonic structure with an embedded 2D array of NPs, we use the transfer matrix formalism. The transfer matrix of the whole structure is obtained through a sequential product of interface matrices and propagation matrices as shown below.

The transfer matrix for an internal interface separating two homogeneous dielectric media with refractive indexes  $n_{j-1}$  and  $n_j$ , involves complex Fresnel reflection ( $r_j$ ) and refraction ( $t_j$ ) coefficients [26]:

$$\hat{I}_j = \frac{1}{t_j} \begin{pmatrix} 1 & r_j \\ r_j & 1 \end{pmatrix}, \quad r_j = t_j - 1 = \frac{n_{j-1} - n_j}{n_{j-1} + n_j}. \quad (2)$$

The transfer matrix for 2D NP array, on the other hand, is expressed in terms of reflection coefficient  $r^{\text{NP}}$ . For the two orthogonal longitudinal (parallel to the  $x$  axis) and transverse (parallel to the  $y$  axis) polarization states, these coefficients and the corresponding interface matrix for the NP array are [27]:

$$\hat{I} = \frac{1}{1+r} \begin{pmatrix} 1 & -r \\ r & 1+2r \end{pmatrix}, \quad r \approx i \frac{k_0 \sqrt{\varepsilon_C}}{2p^2} \alpha, \quad (3)$$

where  $\alpha = V(\varepsilon_p - \varepsilon_C) / (g(\varepsilon_p - \varepsilon_C) + \varepsilon_C)$  is the complex polarizability of an individual spheroidal NP in an external optical field applied along the  $x$ - or  $y$ -axis,  $\varepsilon_p$  is relative permittivity of the NP,  $V = 4\pi a_1 a_2^2 / 3$  is the volume of the NP, and  $g$  is a geometric factor accounting for the influence of the shape of the NP on its induced dipolar moment, with  $g = (1 - \xi^2)^{-1} (1 - \xi(1 - \xi^2)^{-1/2} \arcsin(1 - \xi^2)^{1/2})$  [28].

The optical fields at two adjacent interfaces  $j^{\text{th}}$  and  $(j+1)^{\text{th}}$  surrounding the  $j^{\text{th}}$  homogeneous layer  $j$  are related via the propagation matrix  $\hat{F}_j$  defined as [26]:

$$\hat{F}_j = \begin{pmatrix} \exp(-ik_0 \sqrt{\varepsilon_j} d_j) & 0 \\ 0 & \exp(ik_0 \sqrt{\varepsilon_j} d_j) \end{pmatrix}. \quad (4)$$

Overall, the complex amplitudes of the incident  $E_i$ , reflected  $E_r$ , and transmitted  $E_t$  optical fields are related through the transfer matrix  $\hat{G} = \hat{I}_1 \hat{F}_1 \hat{I}_m \hat{F}_2 \left( \prod_{j=2}^{2N+1} \hat{I}_j \hat{F}_{j,j+1} \right) \hat{I}_{2N+2}$  of the entire structure, with

$$\begin{pmatrix} E_i \\ E_r \end{pmatrix} = \hat{G} \begin{pmatrix} E_t \\ 0 \end{pmatrix}, \quad (5)$$

and the reflectivity and transmittivity of the system are obtained as

$$T = |E_t/E_i|^2 = |\hat{G}_{11}|^{-2}, \quad R = |E_r/E_i|^2 = T |\hat{G}_{21}|^2. \quad (6)$$

These formulas allow to calculate transmittivity and reflectivity spectra of the photonic structure with 2D NP array.

## NUMERICAL RESULTS AND DISCUSSION

For the numerical calculations, the unit cell of the DBR is considered to be formed by TiO<sub>2</sub> (material  $A$ ) and SiO<sub>2</sub> (material  $B$ ), the matrix material of the composite layer  $C$  is the same as that of layer  $B$ , so that  $\varepsilon_C = \varepsilon_B$ . The calculations are carried out taking into account the frequency dispersion of the dielectric permittivity of materials [29,30]. Alternate layers  $A$  and  $B$ , repeated  $N = 10$ , have respective thicknesses  $d_A \approx 47$  nm and  $d_B \approx 73$  nm. These thicknesses provide a photonic bandgap centered at  $\lambda_{br} = 430$  nm wavelength according to Eq. (1).

The 2D NP array is considered to be formed by silver (Ag) NPs. To describe the optical properties of single silver NP, we use the expression of the Drude model [31]:

$$\varepsilon_p(\omega) = \varepsilon_0 - \frac{\omega_p^2}{\omega^2 + i\omega\gamma}, \quad (7)$$

where  $\varepsilon_0 = 5$  is the constant taking into account the contributions of interband transitions of bound electrons,  $\omega_p = 13.5 \cdot 10^{15} \text{ s}^{-1}$  is the plasma frequency, and  $\gamma = 5.5 \cdot 10^{13} \text{ s}^{-1}$  is the relaxation parameter, describing the effective electron scattering rate [32]. For the NPs  $\gamma$  should be replaced by  $\gamma_{NP}$  which results not only from the electron collision rate in the metal, but also from the electron collisions with the particle boundary, so that

$$\gamma_{NP} \approx \gamma + \frac{v_F}{s} \quad (8)$$

with  $v_F = 1.4 \cdot 10^6 \text{ m/s}$  being the Fermi velocity for silver [33]. In Eq. (8)  $s$  is the characteristic radius of NP in the direction of the

external field. Calculations show that the correction taking into account the finite size of the particle leads to a significant variation of the NP permittivity  $\varepsilon$  for  $s < 15$  nm [34,35]. For the geometry under consideration  $s = b$ .

Let us consider the spectral characteristics of the 2D array of spheroidal Ag NPs embedded in an infinite  $\text{SiO}_2$  medium. Here and below, the length  $b$  of equatorial axis of NPs is taken equal to 10 nm. The Figure 2 shows the absorption and transmission spectra for different values of the aspect ratio  $\xi$  between the lengths of the polar and equatorial axes of NPs and for the different values of the interparticle distance  $p$ . The plasmon resonance of the NP array is exhibited by the peak in the absorption spectra and by the deep in the transmission spectra. It can be seen from Figure 2(a) that compared to case of spherical NPs ( $\xi = 1$ ), the resonance wavelength of the NP array exhibits a red shift for the oblate NPs ( $\xi < 1$ ) and a blue shift for the prolate NPs ( $\xi > 1$ ). Figure 2(b) shows that the variation of the interparticle distance  $p$  affects mainly the amplitude of the scattered light wave.

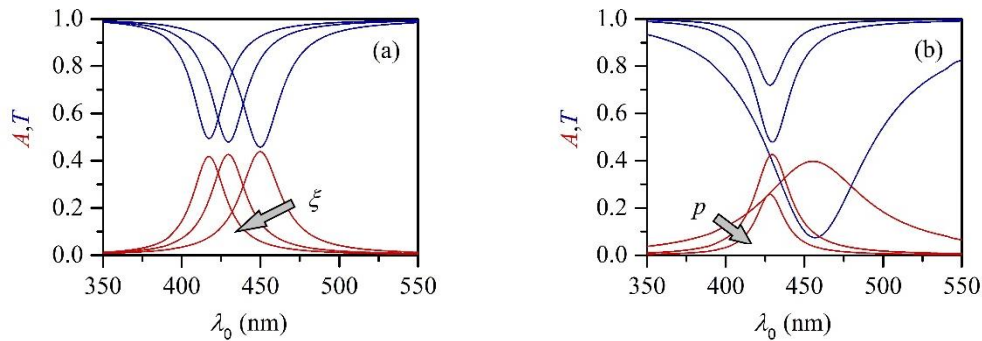


Figure 2. Absorption (red lines) and transmission (blue lines) spectra of the 2D array of Ag NPs embedded in infinite  $\text{SiO}_2$  medium, obtained by analytical method. The parameters of the array of NPs: (a)  $p = 70$  nm,  $\xi = 0.75, 1, 1.25$ ; (b)  $\xi = 1$ ,  $p = 30, 70, 110$  nm. Gray arrows indicate the directions of increasing parameters  $\xi$  and  $p$ .

In order to verify the used analytical method, we compare the results with FEM calculations conducted in COMSOL Multiphysics. The results of analytical calculations and numerical simulations for a wide range of particle-to-interface and interparticle distances are presented in Figure 3. In Figure 3(b) and Figure 3(d), the minimum distance from the array to the interface is 30 nm, which is approximately 9 times less than the resonant wavelength in medium and equal to 3 particle radii. For a considered range of parameters, the results of the analytical and numerical methods are in good agreement. There is a small frequency shift between the spectral lines obtained via different methods.

In the following, we analyze the impact of resonant NPs on the spectral characteristics of a hybrid structure. For this purpose, we consider NP array with fixed parameters  $\xi = 1$  and  $p = 80$  nm. For the adopted parameters, the plasmon resonance of NP array is located near the wavelength 430 nm, and the PBG of DBR covers a range between 375 nm and 500 nm. Thickness of the layer C ( $d_c = d_1 + d_2$ ) is chosen to be equal  $5d_B = 363$  nm.

The results of calculation are presented on Figure 4. Panel (c) shows the absorption spectrum as a function of the relative distance  $1 \leq d_2 / d_B \leq 8$ . One can see that variation of the NP array position changes the spectral characteristics of the entire structure, which results in appearance of the color ‘islands’ corresponding to high absorptivity. The periodicity of the dependence of  $A$  on the thickness  $d_2$  of layer  $C_2$ , which is observed in the region of the wavelength  $\lambda_0 = 430$  nm, is due to the alternation of maxima and minima of the optical field in the longitudinal direction of the structure. Note that near a wavelength of 350 nm the light absorptivity takes on values greater than 0.1 due to absorption in the layers A ( $\text{TiO}_2$ ).

Left panels of Figure 4 demonstrate absorption and transmission spectra for two values of  $d_2 / d_B$ . For  $d_2 / d_B = 3$  the photonic structure completely absorbs the incoming radiation at the LSPR wavelength  $\lambda_0 = 430$  nm. For  $d_2 / d_B = 2$  reflectivity in the PBG takes high values close to 1, i.e. the absorptivity equals 0. In the last case, the reflectivity of the entire structure takes on a value equal to 1 around the wavelength 430 nm despite the presence of light-absorbing NPs. Note, that such a high value of total reflectivity ( $R = 1$ ) is typical for non-absorbing Bragg mirrors, and this means that in the structure  $C_1MC_2[AB]$ <sup>10</sup> the resonant metal NP array  $M$  is “hidden” from the electromagnetic radiation at the wavelength 430 nm.

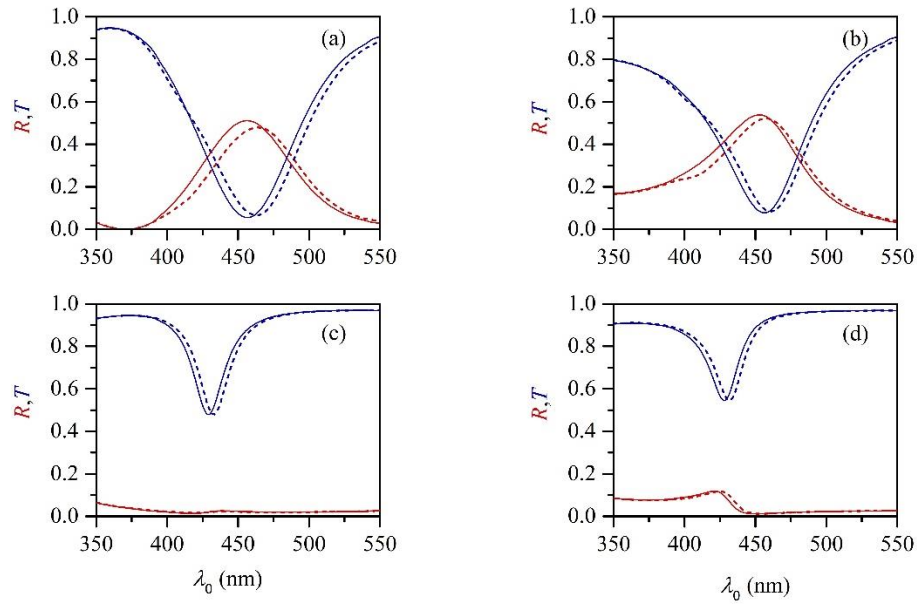


Figure 3. Spectral characteristics of the 2D array of Ag nanoparticles embedded in  $\text{SiO}_2$  medium near the interface with  $\text{TiO}_2$  medium, obtained by analytical method (solid lines) and numerical simulation (dashed lines). Distance between array and the first interface of DBR is (a),(c) 220 nm, (b),(d) 30 nm. The parameters of NP array:  $a = b = 10$  nm, (a),(b)  $p = 30$  nm, (c),(d)  $p = 80$  nm.

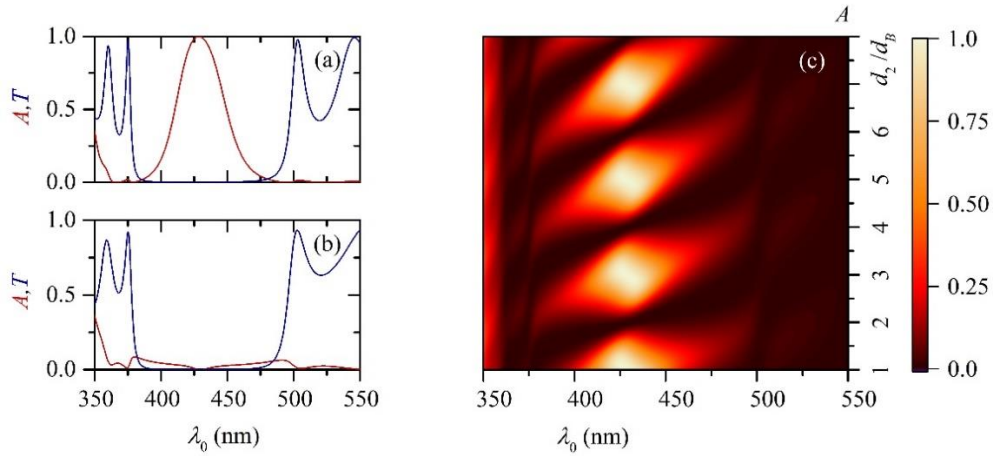


Figure 4. Spectral characteristics of the hybrid structure  $C_1MC_2[AB]^{10}$  (with the 2D NP array). Panels (a) and (b): Absorption (red curves) and transmission (blue curves) spectra for two different distances  $d_2$  between the photonic crystal and the NP array:  $d_2 / d_B = 3$  (a) and  $d_2 / d_B = 2$  (b). Panel (c): Absorption spectrum as a function of the relative distance between the DBR and the NP array.

Figure 5 demonstrates the spectra of the hybrid structure  $C_1MC_2[AB]^{10}$  for different values of interparticle distance and aspect ratio of Ag NPs. Calculations are carried out for the case when NPs are placed in nodes of the optical field in layer C. It is obvious from comparison with Figure 2 that the total spectra are affected mainly by the LSPR of NPs. The change of aspect ratio  $\zeta$  causes a frequency shift of the surface plasmon peak of the NPs and thereby a shift in the absorption spectrum of hybrid structure. As may be seen from Figures 5(c) and 5(d), the simulation results and the predictions of analytical calculations are in good agreement. The main difference between the results obtained by the two methods is the small frequency shift between the spectral lines.

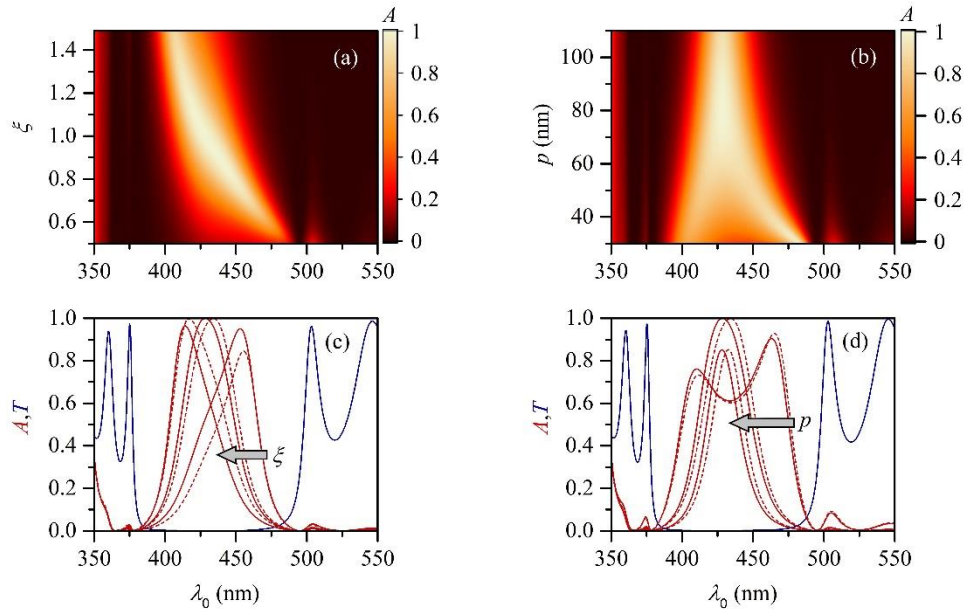


Figure 5. Spectral characteristics of the hybrid structure  $C_1MC_2[AB]^{10}$  (with the 2D NP array). The parameters of the structure:  $d_1 = 2d_B = 145$  nm,  $d_2 = 3d_B = 218$  nm. Panels (a) and (b): Absorption spectra for (a)  $p = 80$  nm, (b)  $\zeta = 1$ . Panels (c) and (d): Absorption (red curves) and transmission (blue curves) spectra obtained by analytical method (solid lines) and numerical simulation (dashed lines) for (c)  $p = 80$  nm,  $\zeta = 0.75, 1, 1.25$ , (d)  $\zeta = 1$ ,  $p = 40, 80, 120$  nm. Gray arrows indicate the directions of increasing parameters  $\zeta$  and  $p$ .

## CONCLUSIONS

In this work, we show that a significant modification of the reflection and absorption spectra of a distributed Bragg reflector (one-dimensional photonic crystal) in the visible spectral region can be achieved by placing of a diluted two-dimensional array of metal NPs inside a dielectric layer adjacent to the Bragg mirror. The complete suppression of the reflection of an electromagnetic wave in the photonic bandgap region is demonstrated. To achieve the effect of the total light absorption, the adjustment of the amplitude and phase of the scattered light waves is required, as well as the correct choice of location of the resonant NP array near the maxima of the resulting electromagnetic field strength inside the surface film. The operating wavelength can be tuned by varying the size and shape of NPs and the interparticle spacing. The proposed absorbers can be used for applications in solar energy harvesting and emission tailoring.

## ACKNOWLEDGEMENTS

The work was carried out within the framework of the state task of the Kotelnikov Institute of Radioengineering and Electronics of Russian Academy of Sciences. A.F. is supported by the European Union's Horizon 2020 research and innovation programme (Individual Fellowship, H2020-MSCA-IF-2020, #101028712).

## REFERENCES

- [1] Noguez, C., "Surface Plasmons on Metal Nanoparticles: The Influence of Shape and Physical Environment," *J. Phys. Chem. C* 111, 3806 (2007).
- [2] Kelly, K. L., Coronado, E., Zhao, L. L., Schatz, G. C., "The Optical Properties of Metal Nanoparticles: The Influence of Size, Shape, and Dielectric Environment," *J. Phys. Chem. B* 107(3), 668–677 (2003).
- [3] Yang, P., Zheng, J., Xu, Y., Zhang, Q. & Jiang, L. "Colloidal synthesis and applications of plasmonic metal nanoparticles," *Advanced Materials* 28(47), 10508–10517 (2016).
- [4] Kunwar, S., Sui, M., Pandey, P. et al., "Improved Configuration and LSPR Response of Platinum Nanoparticles via Enhanced Solid State Dewetting of In-Pt Bilayers," *Sci Rep* 9, 1329 (2019).
- [5] Piella, J., Bastús, N. G. & Puntès, V., "Size-Controlled Synthesis of Sub-10-nanometer Citrate-Stabilized Gold Nanoparticles and Related Optical Properties," *Chem. Mater* 28(4), 1066–1075 (2016).



- [6] Moiseev, S. G., "Nanocomposite-based ultrathin polarization beamsplitter," *Opt. Spectrosc.* 111, 233-240 (2011).
- [7] Oraevsky, A. N., Protsenko, I. E., "Optical properties of heterogeneous media," *Quantum Electron.* 31(3), 252–256 (2001).
- [8] Moiseev, S. G., "Optical properties of a Maxwell-Garnett composite medium with nonspherical silver inclusions," *Russ. Phys. J.* 52, 1121-1127 (2009).
- [9] Etrich, C., Fahr, S., Hedayati, M. K., Faupel, F., Elbahri, M., Rockstuhl, C., "Effective Optical Properties of Plasmonic Nanocomposites," *Materials* 7, 727-741 (2014).
- [10] Moiseev, S. G., Pashinina, E. A., Sukhov, S. V., "On the problems of transparency of metal–dielectric composite media with dissipative and amplifying components," *Quantum Electron.* 37(5), 446-452 (2007).
- [11] Mayer, K. M., Hafner, J. H., "Localized Surface Plasmon Resonance Sensors," *Chem. Rev.* 111, 3828-3857 (2011).
- [12] Moiseev, S. G., "Composite medium with silver nanoparticles as an anti-reflection optical coating," *Appl. Phys. A* 103, 619-622 (2011).
- [13] Shalin, A. S., Moiseev, S. G., "Controlling interface reflectance by a monolayer of nanoparticles," *Quantum Electron.* 39(12), 1175-1181 (2009).
- [14] Hofmeister, H., Drost, W. G., and Berger, A., "Oriented prolate silver particles in glass – characteristics of novel dichroic polarizers," *Nanostruct. Mater.* 12, 207-210 (1999).
- [15] Zhang, F., Liu, B., Tian, Z., Zhu, N., "Pyramid-shaped ultra-stable gold-helix metamaterial as an efficient mid-infrared circular polarizer," *Appl. Phys. Express* 15, 112006 (2022).
- [16] Kravets, V. G., Neubeck, S., Grigorenko, A. N., Kravets, A. F., "Plasmonic blackbody: Strong absorption of light by metal nanoparticles embedded in a dielectric matrix," *Phys. Rev. B*, 81(16), 165401 (2010).
- [17] Dadoenkova, Y., Glukhov, I., Moiseev, S., Svetukhin, V., Zhukov, A. and Zolotovskii, I., "Optical generation in an amplifying photonic crystal with an embedded nanocomposite polarizer," *Opt. Commun.* 389, 1-4 (2017).
- [18] Aly, A. H., Malek, C., Elsayed, H. A., "Transmittance properties of a quasiperiodic one-dimensional photonic crystals that incorporate nanocomposite material," *Int. J. Mod. Phys. B* 32, 1850220 (2018).
- [19] Singh, P., Thapa, K. B., Kumar, N., Singh, D., and Kumar, D., "Effective optical properties of the one-dimensional periodic structure of TiO<sub>2</sub> and SiO<sub>2</sub> layers with a defect layer of nanocomposite consisting of silver nanoparticle and E7 liquid crystal," *Pramana-J. Phys.* 93(3), 50 (2019).
- [20] Moiseev, S. G., Ostatochnikov, V. A., Sementsov, D. I. "Influence of size effects on the optical characteristics of a one-dimensional photonic crystal with a nanocomposite defect," *JETP Letters* 100(6), 371-375 (2014).
- [21] Moiseev, S. G., Ostatochnikov, V. A., "Defect modes of one-dimensional photonic-crystal structure with a resonance nanocomposite layer," *Quantum Electron.* 46(8), 743–748 (2016).
- [22] Mohamed, A. G., Sabra, W., Mehaney, A., Aly, A. H., Elsayed, H. A., "Multiplication of photonic band gaps in one-dimensional photonic crystals by using hyperbolic metamaterial in IR range," *Sci. Rep.* 13, 324 (2023).
- [23] Moiseev, S. G., Glukhov, I. A., Ostatochnikov, V. A., Anzulevich, A. P., Anzulevich, S. N., "Spectra from a photonic crystal structure with a metallic nanoparticle monolayer," *J. Appl. Spectrosc.* 85(3), 511-516 (2018).
- [24] Moiseev, S. G., Glukhov, I. A., Dadoenkova, Y. S., Bentivegna, F. F. L., "Polarization-selective defect mode amplification in a photonic crystal with intracavity 2D arrays of metallic nanoparticles," *J. Opt. Soc. Am. B* 36, 1645-1652 (2019).
- [25] Glukhov, I. A., Dadoenkova, Y. S., Bentivegna, F. F. L., Moiseev, S. G., "Deterministic aperiodic photonic crystal with a 2D array of metallic nanoparticles as polarization-sensitive dichroic filter," *J. Appl. Phys.* 128(5) 053101, (2020).
- [26] Born, M. and Wolf, E., [Principles of Optics], Cambridge University Press, Cambridge (1999).
- [27] Holloway, C. L., Mohamed, M. A., Kuester, E. F. and Dienstfrey A., "Reflection and transmission properties of a metafilm: With an application to a controllable surface composed of resonant particles," *IEEE Trans. Electromagn. Compat.* 47(4), 853–865 (2005).
- [28] Bohren, C. F. and Huffman, D. R., [Absorption and Scattering of Light by Small Particles], Wiley, New York (1983).
- [29] Rodriguez-de Marcos, L. V., Larruquert, J. I., Mindez, J. A., Aznirez, J. A., "Self-consistent optical constants of SiO<sub>2</sub> and Ta<sub>2</sub>O<sub>5</sub> films," *Opt. Mater. Express* 6, 3622-3637 (2016).
- [30] Sarkar, S., Gupta, V., Kumar, M., Schubert, J., Probst, P. T., Joseph, J., König, T. A. F., "Hybridized guided-mode resonances via colloidal plasmonic self-assembled grating," *ACS Appl. Mater. Interfaces* 11, 13752-13760 (2019).
- [31] Kreibig, U., Vollmer, M., [Optical Properties of Metal Clusters], Springer, Berlin (1995).

- [32] Johnson, P. B., Christy, R. W., "Optical Constants of Noble Metals," *Phys. Rev.* 6, 4370-4379 (1972).
- [33] Yannopapas, V., Modinos, A., and Stefanou, N., "Scattering and absorption of light by periodic and nearly periodic metallodielectric structures," *Opt. Quantum Electron.* 34, 227-234 (2002).
- [34] Moiseev, S. G., "Active Maxwell-Garnett composite with the unit refractive index," *Physica B Condens. Matter* 405(14), 3042-3045 (2010).
- [35] Singh, P., Kumar, V., Janma R., and Thapa, K., "Theoretical investigation of enhanced sensing property in 1D TiO<sub>2</sub>/SiO<sub>2</sub> periodic layers containing a defect layer of the nanocomposite with different radii of silver nanoparticles in the host liquid crystal," *Phys. Scr.* 95, 065507 (2020).